SRTTU

JCARME
ISSN: 2228-7922
Journal of Computational and Applied Research in Mechanical Engineering
Vol. x, No. x, xxxx
jcarme.sru.ac.ir

Effect of axial groove location, length & width ratio on the bearing properties and stability

Vijay Kumar Dwivedi[a*], Pooja Pathak[b]

[a]*Department of Mechanical Engineering, GLA University, Mathura (U.P), 201406, INDIA*
[b]*Department of Mathematics, GLA University, Mathura (U.P), 201406, INDIA*

Nomenclature

a	Groove length
C/R	Clearance ratio
D	Diameter of bearing
h	Film thickness
$\overline{K}_{\alpha}$, $\overline{K}_{\beta}$	Non dimensionalized turbulence coefficients in X, Y direction
L	Bearing length
P_s	Supply pressure
S_n	Sommerfeld number
w	Width of groove
$\dot{X}_j, \dot{Z}_j$	Journal centre velocity
λ	Aspect ratio (L/D)
α_g	Location of groove
Ω	Rotational velocity of journal
μ	Lubricant Viscosity

Abstract

There are many industrial application of axial grooved journal bearing especially in turbo machinery. The stability is a very big issue for researcher, in high speed rotating machines. The axial groove journal bearing have a capacity to reduce the vibration and ability to resolve the heating problems as well as stability at higher speed. Dynamic performance parameters and stability of axial grooved hybrid journal bearings depend on the dimensions and orientations of groove in a great extent at higher speeds. In this work, a FORTRAN program has been used to solve Reynolds governing equation. The bearing performance characteristics have been simulated for the various dimensions and orientation of groove. Non linear journal centre trajectories are drawn for different Reynolds number for stability analysis. It has been found that the smaller groove length has resulted in lower bearing capacity whereas smaller groove width yielded higher bearing capacity and the turbulence decreases the stability. The groove location also strongly affects most performance parameter. The optimum location of groove axis was obtained between 60^0 to 90^0 to the load line.

Keywords:

Axial Groove; Damping Coefficient; Stiffness Coefficient; Stability.

1. Introduction

In turbo-machinery with high loads and high journal speeds are widely used hybrid bearings. The lubricant is often delivered through one or two grooves at a prescribed pressure from a supply hole at the inlet. Groove dimensions and their number have significant effect on bearing performance. These grooves are cut into the inner surface of t he bearing. Depending on the application, the gr

[*]*Corresponding author*
Email address: vijay.dwivedi@gla.ac.in

oove configuration can be axial, circumferential and spiral.Usually, the groove is located at 90^0 on the load line, upstream of the minimum film thickness position.

O'Donoghue and Rowe [1968 ; 1969] developed an externally pressurized bearing design method based on pad load and flow coefficients that depend only on the geometric shape and proportions of the bearing and are independent of the control device used.

They also gave the exact procedure together with the Reynolds equation's computer solution for a finite hydrostatic multirecess bearing using a finite difference method. Koshal *et al.* [1981] also analyzed the effect of a/L ratio on load bearing capacity. They concluded that the load bearing capacity is increased with increase in power ratio (K) for same a/L ratio. Andres and Szeri [1984] present the analytical solution for flow between eccentric rotating cylinders. Mortonet et al. [1987] presented grooves ' Effect on rotating system stability and response. They found that grooved bearing modifies the locus of the journal by increasing the angle of attitude and also changes the boundary of cavitation at low ratios of excentricity, i.e. high speeds.

Gethin and Deihi [1987] used the finite element method to study the effect of loading direction on the performance of a twin axial groove bearing. They concluded that when the grooves were orthogonal to the load line, the load carrying capacity was optimal.

Sinhasan and Chadrawat [1988] showed bearing properties for many deformation coefficient values and Reynolds number of two axial groove journal bearings operating in laminar and superlaminar flow regimes. Basri and Neal [1990] were the first to include a separate flow rate measurement at each groove. Pai and Mazumdar [1991] discussed the stability properties of submerged, unidirectional plain journal bearings under a constant and variable rotating load. Claro and Mirinda [1993] studied the journal bearing characteristics by considering the lubricant suppy conditions. Mishra and Kumar [1996] presented the effects of geometric change on stability of hydrodynamic journal bearing due to wear. They concluded that the stability decreases due to wear of journal or bearing. Mishra and Kumar [1996] also analyzed the steady state behavior of non-circular worn journal bearing. They observed that geometric change caused by wear has a significant effect on the steady state characteristics of bearing. KaKoty and Mazumdar [2000] studied the effect of fluid inertia on stability of oil journal bearings. They attempted to evaluate the mass parameter (measure of stability) besides finding out steady state characteristics of finite journal bearings considering the effect of inertia. Jerry and Su [2001] investigation the rotation effect hybrid bearing. Costa *et al*. [2003] investigate that one groove (located at load line) bearing has better perform. They also commented that twin groove journal bearing are widely used especially when the shaft is expected to assume both direction of rotation. Majumdar *et al.* [2004] obtained steady state and dynamic characteristics including whirl instability of water lubricated journal bearing having three axial grooves theoretically. Desai *et al.* [2005] carried out an analysis of pressure distribution of hydrodynamic journal bearings with different groove configuration. They suggested the use of circumferential groove at the centre of bearing, with an oil supply hole located opposite the load bearing zone. Brito *et al*. [2006; 2007] have investigated experimentally the Effect of supply temperature, pressure and load applied on the performance of a journal bearing. *Brito et al.* concluded that the increment in feeding pressure resulted in an increase in oil flow rate, a reduction in oil temperature and a slight increase in the angle of attitude and a minimum film thickness. Kini *et al*. [2009] investigated the effect of groove location on the dynamic characteristics of multiple axial groove water lubricated journal bearing. They obtained the stability characteristics of water lubricated journal bearing having three axial grooves theoretically and obtained stiffness and damping coefficient for various bearing number and eccentricity ratio. Roy and Laha [2009] investigated the steady state and dynamic characteristics of axial grove journal bearing. Mehta *et al*. [2010] further extended their work by using couple stress lubricant for the stability of two lobe hydrodynamic bearing. Navthar and Halegowda [2010] presented a method to

determine the synchronous whirl i.e. stability of hydrodynamic journal bearings by using dynamic characteristics such as stiffness coefficients. Roy and Kakoty [2013] presents the various arrangements of grooving location of two groove oil journal bearing for optimum performance. Brito et al.[2014] prestented a thermohydrodynamic (THD) model for performance enhancement and friction reduction analysis of journal bearings with realistic feed condition.. Dwivedi *et al*. [2013; 2014; 2016] has studied the effect of flow regime and recess shape on the static dynamic performance of hydrostatic & hydrodynamic bearing. They also carried the stability analysis of the journal bearing in different flow regimes.Wang et al. [2018] discussed the effect of geometry parameters on the load capacity & friction coefficient of the bearing. They concluded that bearing load capacity is reduced by the concave spherical texture, but enhanced by the convex texture, whereas the surface textures have very slight Effect on friction coefficient. Sharma and Awasthi [2018] have theoretically investigated the effect of transient wear on the performance of hydrodynamic bearing. They have concluded that effect of wear on all static and dynamic parameters increased with increase in eccentricity ratio.

2. Theoretical Model/Analysis

Theoretical model was developed for the analysis of static and dynamic characteristics of two groove journal bearing.

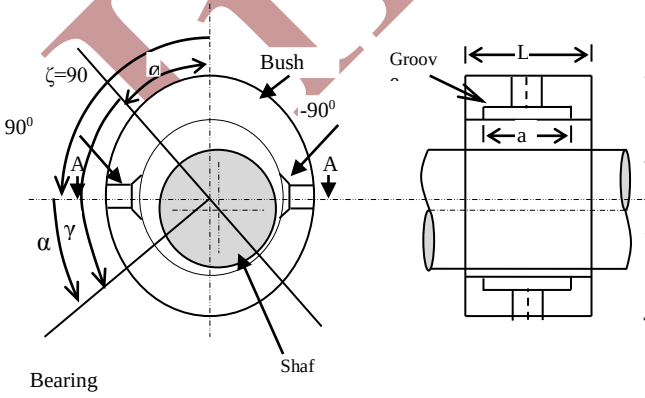

Fig. 1. Journal bearing configuration

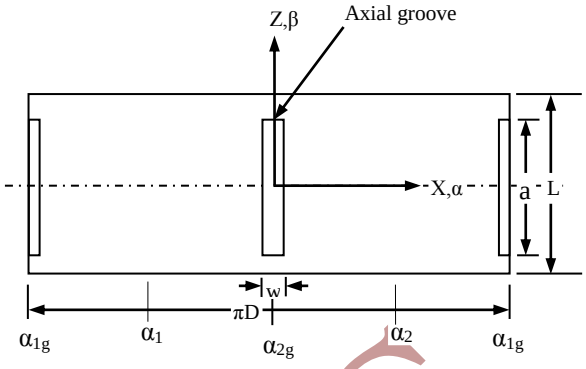

Fig. 2. Coordinate system of unwrapped bearing with fluid domain

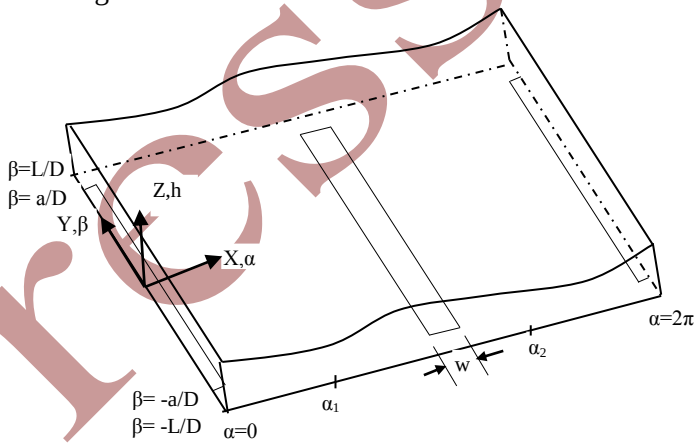

Fig. 3. Three dimensional view of fluid film between journal and bearing

Fig 1 shows the journal bearing configuration. Fig 2 and Fig. 3. show the Coordinate system of unwrapped bearing with fluid domain in 2-D 3-D respectively, considering very small fluid film thickness. α_1 and α_2 as shown in Fig 2 & 3 represent positive fluid film pressure whereas location of centre line of the grooves represent by α_{1g} and α_{2g} respectively.

2.1. Flow field equation

Constatantinescu (1967) presented linearized turbulence theory which governs the flow of lubricating oil in the clearance space between journal and bearing surface. He gave dimensionless Reynolds equation which is given by Eq. (1)

$$\frac{\partial}{\partial\alpha}\left[\frac{\bar{h}^3}{\bar{\mu}\bar{K}_\alpha}\frac{\partial\bar{p}}{\partial\alpha}\right]+\frac{\partial}{\partial\beta}\left[\frac{\bar{h}^3}{\bar{\mu}\bar{K}_\beta}\frac{\partial\bar{p}}{\partial\beta}\right]=\frac{1}{2}\bar{\Omega}\left(\bar{X}_j\sin\alpha-\bar{Z}_j\cos\alpha\right)-\dot{\bar{X}}_j\cos\alpha-\dot{\bar{Z}}_j\sin\alpha \quad (1)$$

The dimensional less thickness of fluid film ($\bar{h}$) is given by

$$\bar{h}=1-\bar{X}_j\cos\alpha-\bar{Z}_j\sin\alpha \quad (2)$$

2.1.1. Approximation of short bearing

Bearing is infinitely short is assumed in short bearing approximation concept so that pressure gradient is very very less in the circumferential direction as compared to axial direction, i.e.

$$\frac{\partial p}{\partial\alpha}\ll\frac{\partial p}{\partial\beta}$$

The Reynolds Equation reduces to

$$\frac{\partial}{\partial\beta}\left[\frac{\bar{h}^3}{\bar{\mu}\bar{K}_\beta}\frac{\partial\bar{p}}{\partial\beta}\right]=f(\alpha) \quad (3)$$

where $f(\alpha)=\frac{1}{2}\bar{\Omega}\left(\bar{X}_j\sin\alpha-\bar{Z}_j\cos\alpha\right)-\dot{\bar{X}}_j\cos\alpha-\dot{\bar{Z}}_j\sin\alpha$ (4)

Eq. (3) is solved using boundary conditions as discussed in section 2.2.

2.2. Boundary conditions (B.C.)

The B. C. used to the current work are given below

(i) $\frac{\partial\bar{p}}{\partial\beta}=0$ at $\beta=0$ (ii) $\bar{p}=0$ at $\beta=\pm\frac{L}{D}=\pm\lambda$ (5a)

(iii) $\bar{p}=0$ at $\left(\left(-\frac{a}{D}<\beta<\frac{a}{D}\right)\right.$ and $\left.\left((\alpha_{1g}-\frac{w}{D})<\alpha<(\alpha_{1g}+\frac{w}{D})\right)\right)$ (5b)

(iv) $\bar{p}=0$ at $\left(\left(-\frac{a}{D}<\beta<\frac{a}{D}\right)\right.$ and $\left.\left((\alpha_{2g}-\frac{w}{D})<\alpha<(\alpha_{2g}+\frac{w}{D})\right)\right)$ (5c)

Where α_{1g} and α_{2g} are the center lines of the angular position of grooves in radian

By integrating Eq. (3) w.r.t. β and using B.C., Eq. (5) pressure distribution around the journal is obtained as

$$\bar{p}(\alpha,\beta)=\left(\frac{\bar{\mu}\bar{K}_\beta}{\bar{h}^3}\right)\left(\frac{1}{2}f(\alpha)(\beta^2-\lambda^2)\right) \quad (6)$$

2.3. Load bearing capacity

Journal bearing load carrying capacity of is calculated by double integrating the pressure over the positive pressure zone in axial and circumferential direction. Bearing capacity in X-direction (i.e. circumferential) is represent as

$$\bar{F}_X=-\int_{-\lambda}^{\lambda}\int_{\alpha_1}^{\alpha_2}\bar{p}.\cos\alpha\,d\alpha.d\beta \quad (7)$$

and similarly Bearing capacity in Z direction (i.e.radial) is represent as

$$\bar{F}_Z=-\int_{-\lambda}^{\lambda}\int_{\alpha_1}^{\alpha_2}\bar{p}.\sin\alpha\,d\alpha.d\beta \quad (8)$$

By using Gauss-Legendre integration method equations (7) and (8) are solved numerically over positive pressure zone.

2.4. Computation of fluid film stiffness and damping co- efficient

Fluid film stiffness and damping co-efficients have been obtained numerically by derivatives of fluid film force with respect to journal center and journal velocity component in axial and circumferential direction respectively.

3. Computational procedures/ Numerical model

Lubricant flow Governing equation between bearing and journal (i.e. Reynolds equation) is modified to study the different flow regimes (laminar, transition and turbulent flows), by including turbulence coefficients $\bar{K}_X$ and $\bar{K}_Y$. In this study Reynolds equation has been solved by using short bearing approximation. The closed form pressure expression has been obtained by integrating twice the Reynolds equation and using boundary conditions (as mentioned in Section 2.2) i.e. the bearing pressure at the mid plane is maximum and the pressure at the end of bearing is zero. Only positive pressure zone is taken during the pressure calculation. Pressures below atmospheric and entire groove area are not considered. A computer program with boundary conditions was developed with help of the McCormick et al. [1992].

Result and discussion

Pressure profile, load bearing capacity, fluid film stiffness coefficients and damping coefficients are calculated with help of analysis and solution algorithm. Developed numerical model (computer program) calculated all bearing performance parameters by taking length-diameter ratio (L/D) 0.5 and 0.25. with assumptions such as parallel bearing and journal axes and clearance ratio 0.001 (C/R = 0.001).

3.1. Validation of results

Validity of analysis, solution algorithms and the developed computer model is established by comparing the dimensionless load capacity for different groove locations obtained from the present short bearing approximation with results available in literatures of Gethin and Deihi (1987), Kumar and Mishra (1996) , Brito et al. (2014) and Sharma and Awasthi (2018).

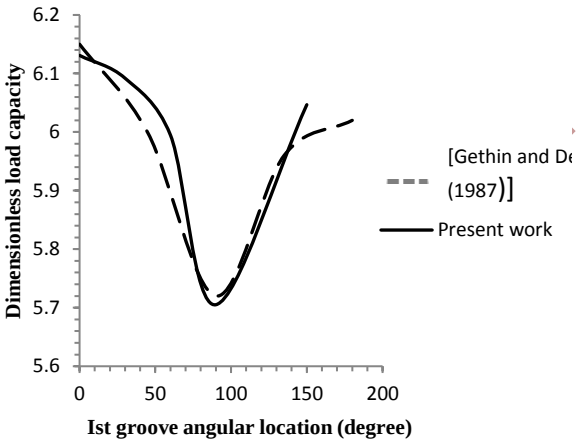

Fig. 4a. Non dimensionalized load capacity Vs groove location

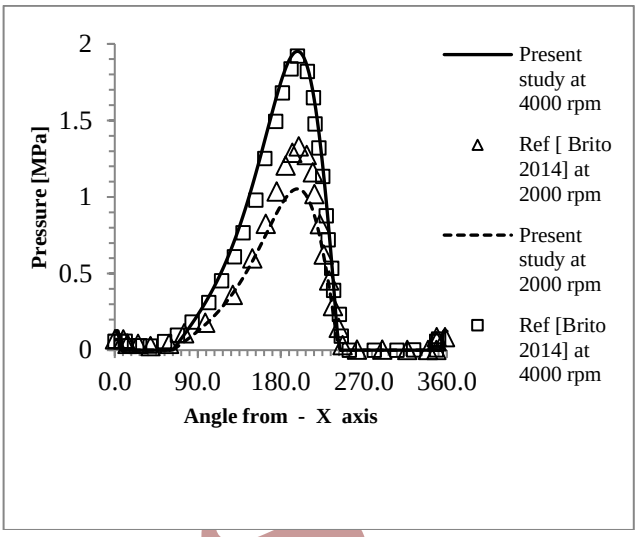

Fig. 4b. Comparison of pressure profile of the bearing between present analysis and experimental data of Brito et al. (2014)

In Fig. 4a, the comparison of nondimensionlized load bearing capacity with different groove location is shown for laminar flow condition with aspect ratio of 0.50, clearance ratio of 0.004 and eccentricity of 0.7 between authors work and available results of Gethin and Deihi (1987) In Fig 4b, the comparison of circumferential pressure with angular location from -X axis is shown for aspect ratio of 0.50, clearance ratio of 0.001 and speed 2000 rpm & 4000 between authors work and available results of Brito et al. (2014).

Figs 4c graphically explained the variations of eccentricity ratio (e) and attitude angle with Sommerfeld number (Sn) at Reynolds number=5000 , aspect ratio of 1.0, wear depth of 0.0 and clearance ratio of 0.001. Results compare well within the acceptable variations due to different methodologies of solution with the results of Sharma and Awasthi (2018) and Kumar and Mishra (1996).

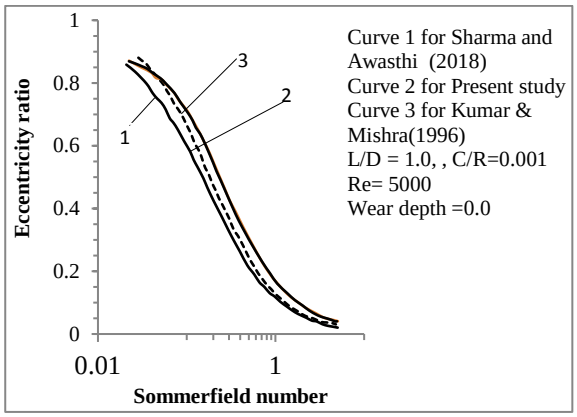

Fig.4c. Eccentricity ratio Vs Sn for aspect ratio = 0.50 for variation of Re

3.2. Effect of the a/L on dimensionless direct stiffness coefficient

The variation of direct stiffness coefficients ($\overline{K}_{XX}, \overline{K}_{XZ}, \overline{K}_{ZX}, \overline{K}_{ZZ}$) with a/L are shown in Figs. 5-8. It is seen from Fig. 5. and Fig. 6. that direct stiffness coefficients in X and Z direction reduces linearly with increment in a/L. The magnitude of cross-coupled damping coefficient Z-X direction is negative over the entire range of a/L.

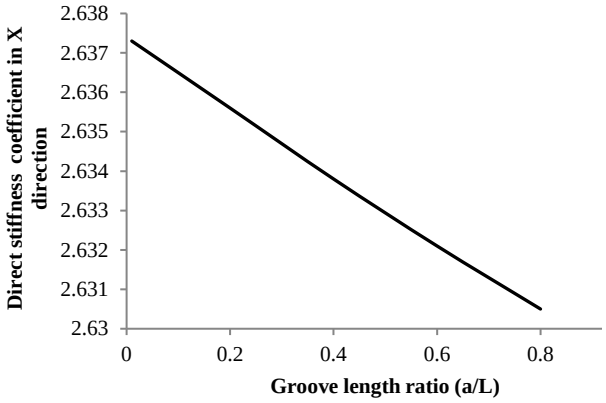

Fig. 5. Effect of a/L on, $\overline{K}_{XX}$

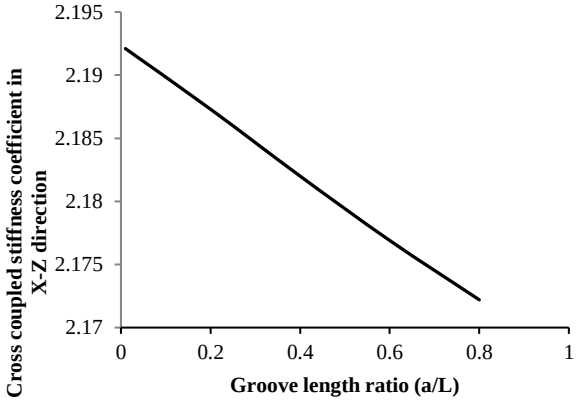

Fig. 6. Effect of a/L on $\overline{K}_{XZ}$

It is seen from Fig. 7. that $\overline{K}_{ZX}$ first reduces with increment in a/L then stabal at a fixed value. The minimum value of $\overline{K}_{ZX}$ = 4.13. Fig. 8 shows direct stiffness in Z direction. As Fig 8 the similar trend is found to the $\overline{K}_{ZX}$ i.e. first it reduces before settling to a fixed value.

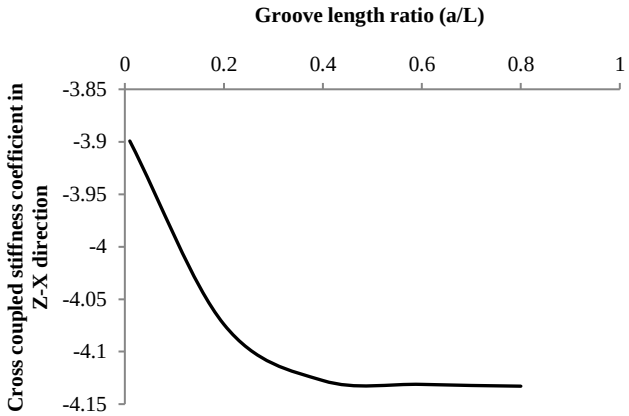

Fig. 7. Effect of a/L on $\overline{K}_{ZX}$

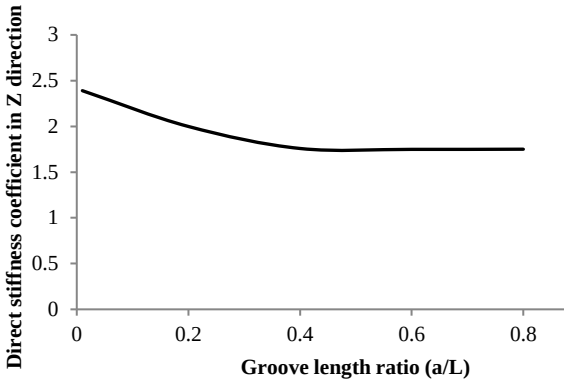

Fig. 8. Effect of a/L on $\bar{K}_{ZZ}$

3.3. Effect of the a/L on direct and cross coupled damping coefficient

Figs. 9 to 11 show the stiffness coefficients ($\bar{C}_{XX}, \bar{C}_{XZ}, \bar{C}_{ZZ}$) are shown in for variation in a/Lwith fixed w/D ratio of 0.02. It is observed from Fig 9 that the direct damping coefficients in X direction, $\bar{C}_{XX}$ increases with increase in a/Lbefore settling to a fixed value. Whereas, direct damping coefficient in Z direction $\bar{C}_{ZZ}$, as shown in Fig. 11, initially decreases up to a/L= 0.17 then increases before settling to a fixed value with increase in a/L.

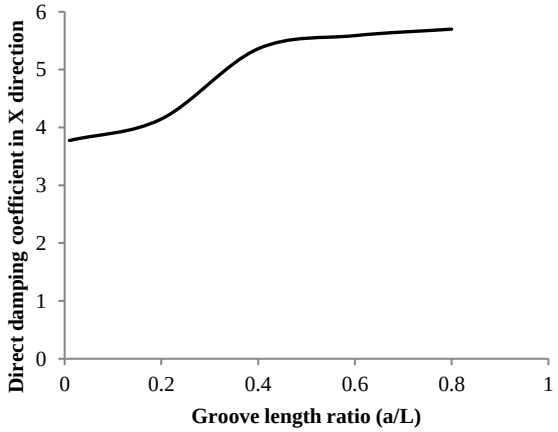

Fig. 9. Effect of a/L on $\bar{C}_{XX}$

Damping coefficients in Z-X direction reduces with increment in a/L before settling. From Fig. 9 to 11 it is concluded that a/L ratio has significant effect on damping co-efficients upto a/Lof 0.4. Thereafter, it not affects the damping co-efficients.

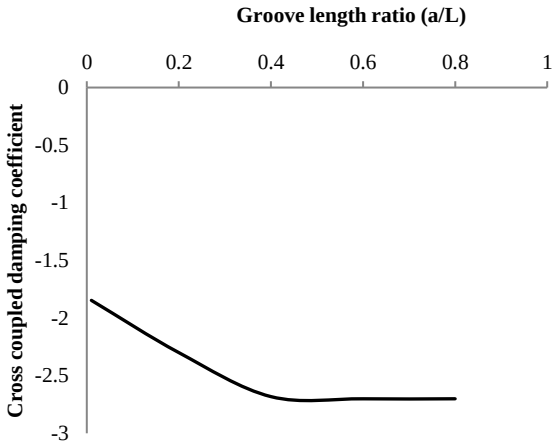

Fig. 10. Effect of a/L on, $\bar{C}_{XZ}$

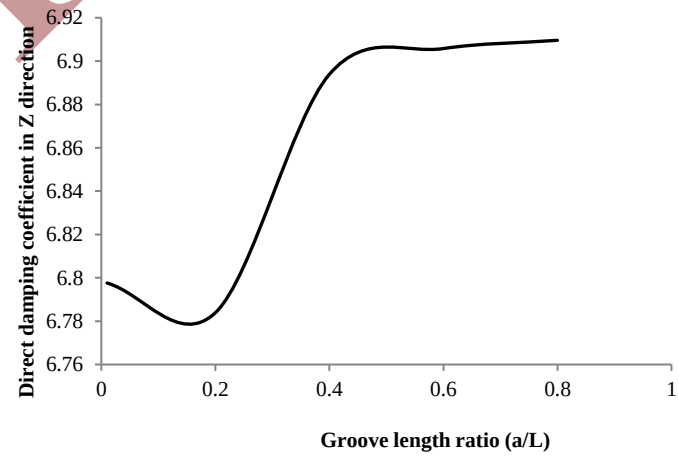

Fig. 11. Effect of a/L on $\bar{C}_{ZZ}$

3.4. Effect of the w/D on stiffness coefficient

Figs. 12 to 15 show the effect of the w/D on stiffness coefficient. It is seen from Fig. 12. that $\bar{K}_{XX}$ is fixed up to w/D = 0.10 then reduces with increment in w/D. Fig 13 shows that $\bar{K}_{XZ}$ reduces with increment in w/D before stabilizing to a fixed value. The lowest value of $\bar{K}_{XZ}$ = 1.43. It is seen from Fig. 14. that $\bar{K}_{ZX}$ increases with reduction in w/D.

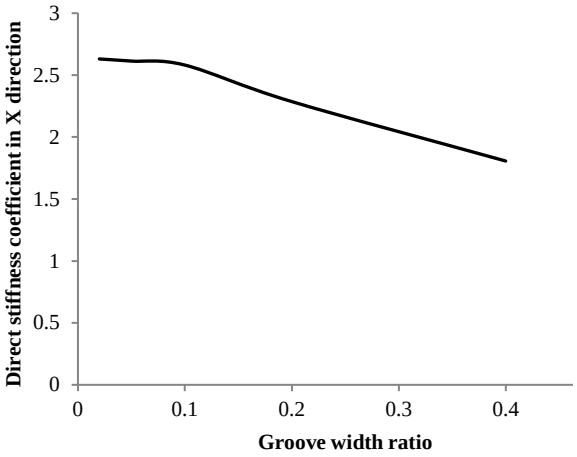

Fig. 12. Effect of w/D on $\bar{K}_{XX}$

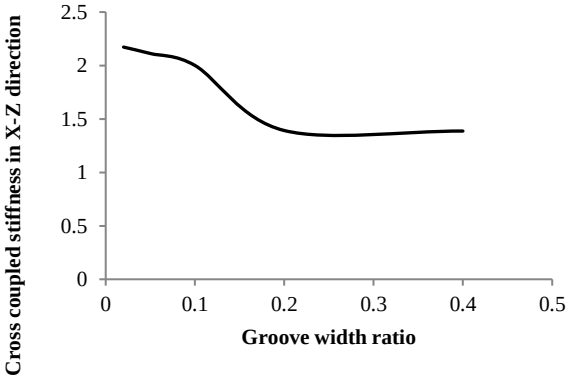

Fig. 13. Effect of w/D on $\bar{K}_{XZ}$

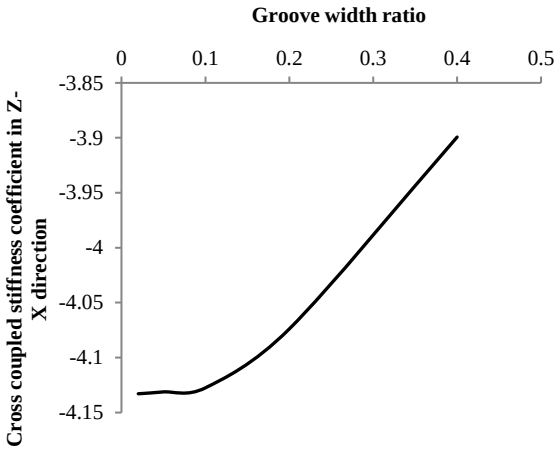

Fig. 14. Effect of w/D on $\bar{K}_{ZX}$

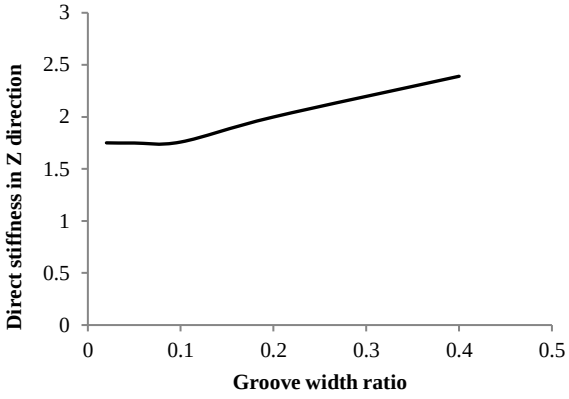

Fig. 15. Effect of w/D on $\bar{K}_{ZZ}$

Fig 15 shows that $\bar{K}_{ZZ}$ is fixed initially up to w/D = 0.10 then increases with increment in w/D.

3.5. Effect of the w/D on damping coefficient

Figs. 16 to 18 show the effect of the w/D on direct and cross-controlled stiffness coefficient ($\bar{C}_{XX}, \bar{C}_{XZ}, \bar{C}_{ZZ}$). Direct damping coefficient in X direction $\bar{C}_{XX}$ reduces with increment in w/D before settling to a certain point. The rate of decrement is highest between w/D = 0.1 and w/D = 0.2. The direct damping co-efficient in Z direction $\bar{C}_{ZZ}$ reduces with increment in w/D upto 0.2. Thereafter, it starts increasing with increase in w/D ratio. Rate of decrement is maximum between w/D ratio of 0.1 to 0.2, similar to the trend for $\bar{C}_{XX}$. The value of cross $\bar{C}_{XZ}$ and $\bar{C}_{ZX}$ are not positive for all groove width ratio. It is seen from Fig. 17 that the $\bar{C}_{XZ}$ is initially fixed up to w/D = 0.1 after that $\bar{C}_{XZ}$ increase with increment with w/D..

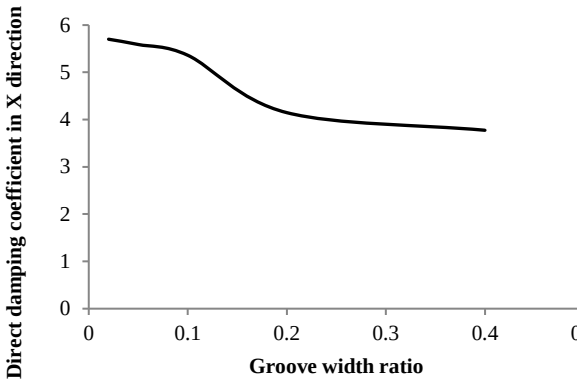

Fig. 16. Effect of w/D on $\bar{C}_{XX}$

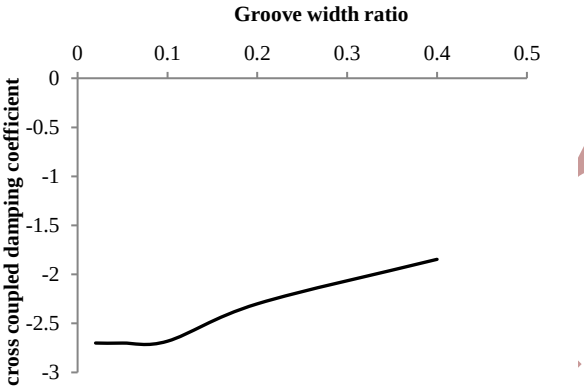

Fig. 17. Effect of w/D on ($\bar{C}_{XZ}$= $\bar{C}_{ZX}$)

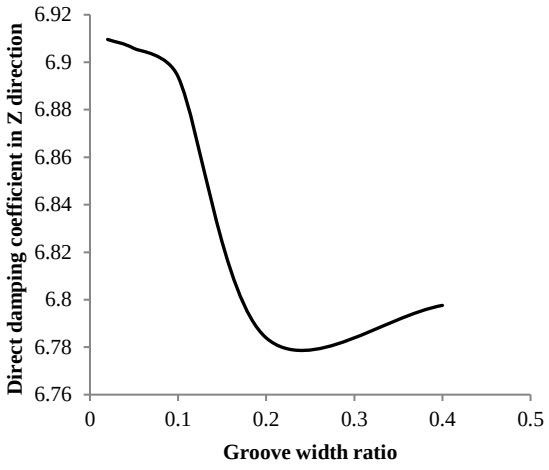

Fig. 18. Effect of w/D on $\bar{C}_{ZZ}$

3.6. Effect of radial position of the axial grooves on stiffness coefficient

Figs. 19-22 shows the variation of $\bar{K}_{XX}, \bar{K}_{XZ}, \bar{K}_{ZX}, \bar{K}_{ZZ}$ with radial position of Ist groove. The position of Ist groove is 180^0 earlier to IInd groove. Fig 34 showed that the variation of $\bar{K}_{XX}$ increment with increment in radial position of Ist groove upto α_{1g} equal to 90^0. An best value of Ist groove radial position $\alpha_{1g}= 90^0$ is seen at which direct stiffness coefficient is highest, i.e. $\bar{K}_{XX} = 2.829$.

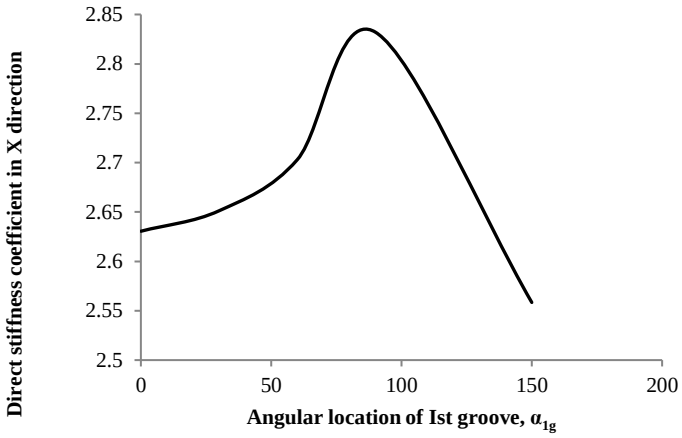

Fig. 19. Effect of radial position of groove on $\bar{K}_{XX}$

The indirect stiffness coefficient $\bar{K}_{XZ}$ is shown in Fig. 20.

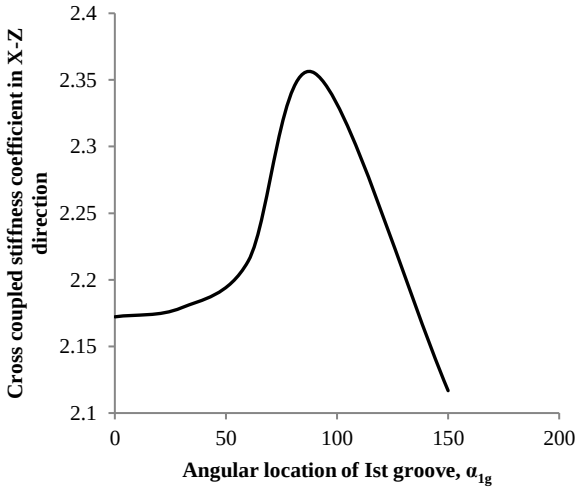

Fig. 20. Effect of radial position of groove on $\bar{K}_{XZ}$

The similar behavior has been seen in the case of $\bar{K}_{XX}$ with Sn. The best value of indirect stiffness $\bar{K}_{XZ}$ is 2.349 at 90^0 of Ist groove angular position. The value of indirect stiffness coefficient $\bar{K}_{ZX}$ is not positive for the whole range of angular position,which is clearly shown in Fig. 21. The variation of $\bar{K}_{ZZ}$ against angular position of Ist groove of two axial groove bearing is shown in Fig. 22. It is seen that $\bar{K}_{ZZ}$ reduces up to $\alpha_{1g} = 90^0$ then increasing behavior is seen up to $\alpha_{1g} = 150^0$.

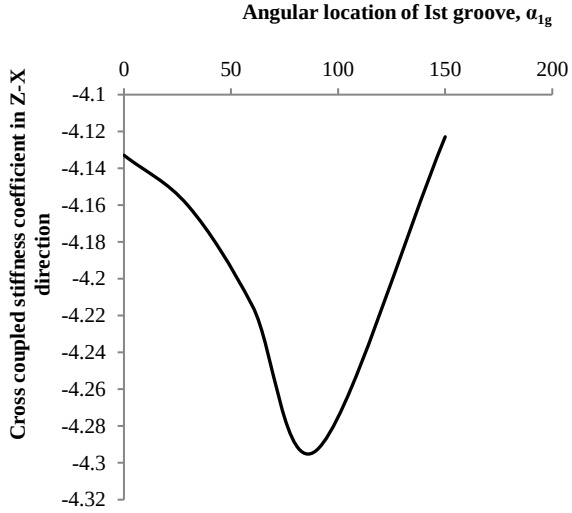

Fig. 21. Effect of radial position of groove on $\bar{K}_{ZX}$

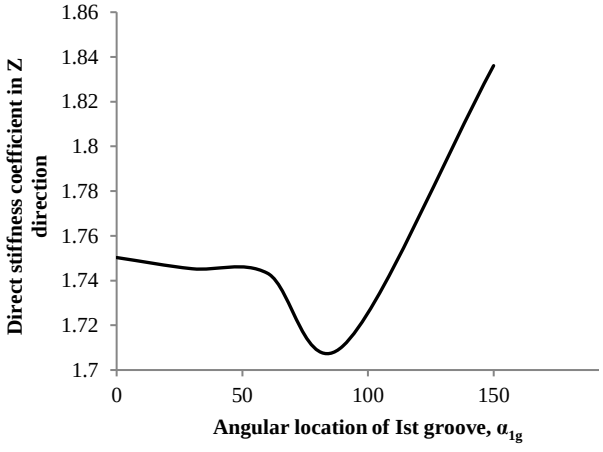

Fig. 22. Effect of radial position of groove on $\bar{K}_{ZZ}$

3.7. Effect of radial position of the grooves on $\bar{C}_{XX}, \bar{C}_{XZ}, \bar{C}_{ZZ}$

Figs 23-25 show the behavior of $\bar{C}_{XX}, \bar{C}_{XZ}, \bar{C}_{ZZ}$ with groove radial position.

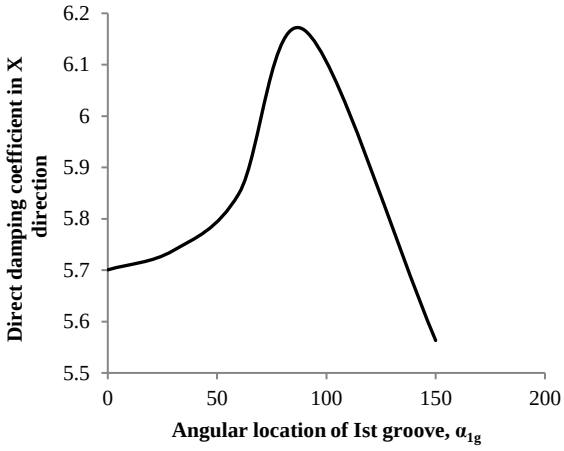

Fig. 23. Effect of radial position of groove on $\bar{C}_{XX}$

The variation of $\bar{C}_{XX}$ is shown in Fig. 23 against radial position of Ist groove radial position, α_{1g} for two axial groove journal bearing. Direct damping coefficient $\bar{C}_{XX}$ increases with increment in radial position of the Ist groove and then reduces. The best value of $\bar{C}_{XX} = 6.167$ at $\alpha_{1g} = 90^0$.

The exact value of indirect damping coefficient $\bar{C}_{XZ} (= \bar{C}_{ZX})$ is not positive for the all values of radial position, Fig 24. The absolute maximum value of $\bar{C}_{XZ} = \bar{C}_{ZX}$ is equal to -2.903 at $\alpha_{1g} = 90^0$. The similar behavior has been seen by $\bar{C}_{ZZ}$ (Fig 25) as observed in the case of $\bar{C}_{XX}$. The best value of $\bar{C}_{ZZ} = 7.129$ at $\alpha_{1g} = 90^0$.

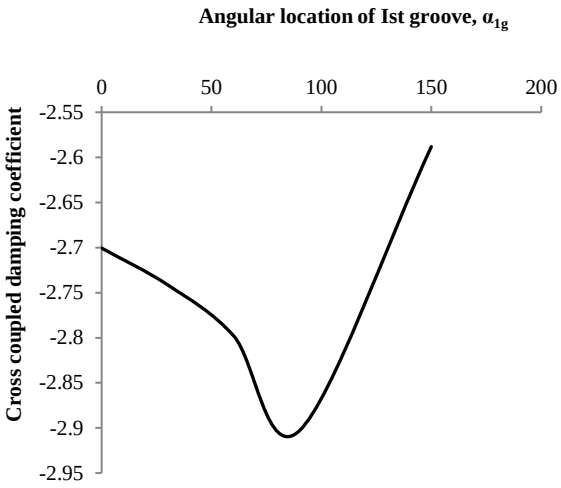

Fig. 24. Effect of radial position of groove on $\bar{C}_{XZ}$

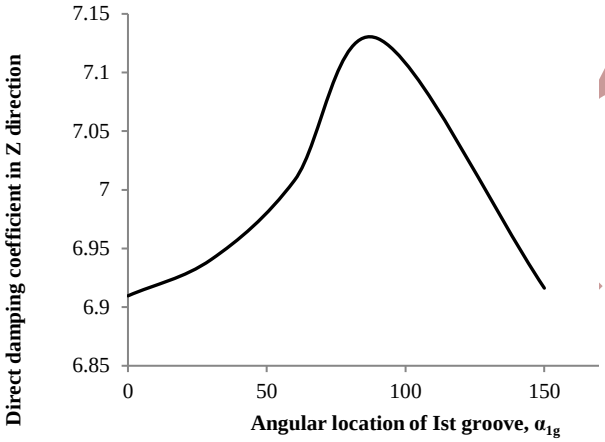

Fig. 25. Effect of radial position of groove on $\bar{C}_{ZZ}$

4. Stability Analysis

Figure 26 shows the stability chart for the analysis of linearized stability under non-laminar and laminar fluid flow conditions of the two axial groove journal bearing. Fig 26 plotted between characteristic speed and Sommerfeld number for non-laminar and laminar fluid flow conditions.

The value of aspect ratio is takes as 0.5 by the author in this study. The obtained trend shows the decrement in characteristic speed for different flow regimes increment in Sommerfeld number and becomes independent of Sommerfeld number for high Sommerfeld number for all flow conditions.

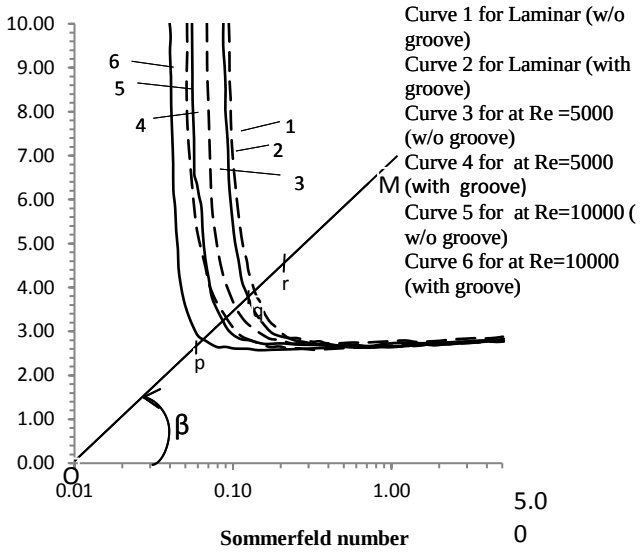

Fig. 26. Comparison chart of characteristic speed for with groove and without groove journal bearing

Table 1. Value of Sn (Sommerfeld number) for different point (p, q, r) on OM line of Fig 26

Operating point	p	q	r
Sommerfeld No.	0.053	0.11	0.17

The validation of linearized analysis stability results were drawn for laminar and superlaminar flow conditions along β-line 'OM' shown in Fig. 26. Value of Sn (Sommerfeld number) for different point (p, q, r) on OM line are given in Table 1.

At fixed velocity of operation with disturbance in displacement $\Delta X_j = \Delta Z_j = 0.005$, the path of bearing shaft centre is shown in Fig. 27 to 28. In this study no velocity disturbance is taken (i.e. $\Delta \dot{X}_j = \Delta \dot{Z}_j = 0$). In this study three operating points 'p', 'q' and 'r' is taken for three different flow regimes.

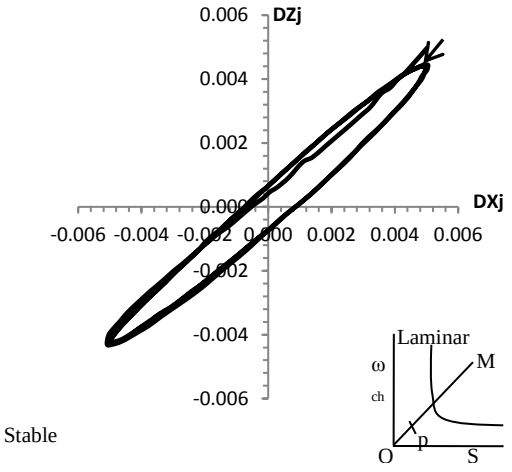

Fig. 27. Path of bearing shaft centre with Nonlinearity with fixed velocity along OM line (Laminar flow, L/D = 0.5, Sn = 0.053, at point 'p'

Bearing shaft (journal) is stable at point 'p' for all flow regimes (i.e. laminar and turbulent both) as shown in Fig. 27 and Fig. 28. It is clearly seen from Fig. 29 the shaft is stable at the point 'q' in laminar region but it becomes

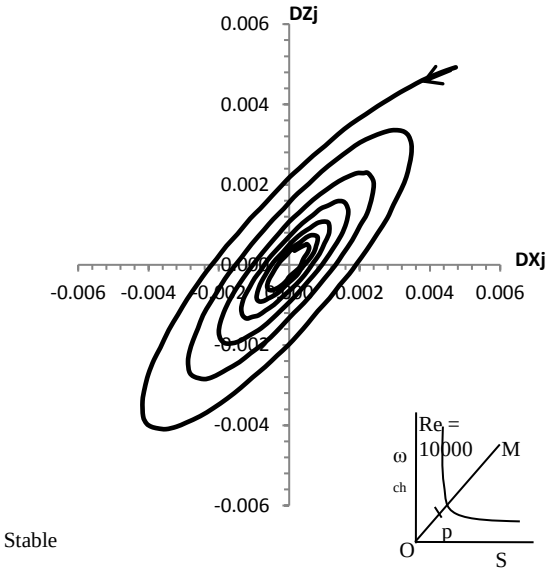

Fig. 28. Path of bearing shaft centre with Nonlinearity with fixed velocity along OM line (Re= 10000, L/D = 0.5, Sn= 0.053, at point 'p') unstable under turbulence flow condition, Fig 30. Whereas it is clearly observed that at point 'r' the journal is always unstable in all flow regimes (i.e. laminar and turbulent regimes, Fig. 31. and Fig. 32.)

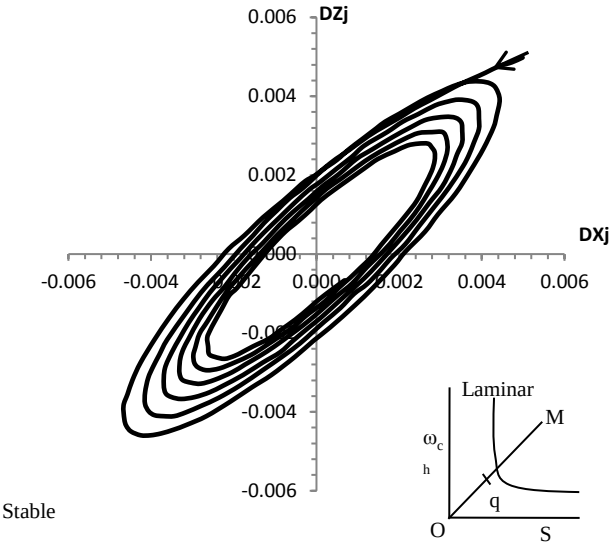

Fig. 29. Path of bearing shaft centre with Nonlinearity with fixed velocity along OM line (Laminar flow, L/D = 0.5, Sn =0.11, at point 'q'

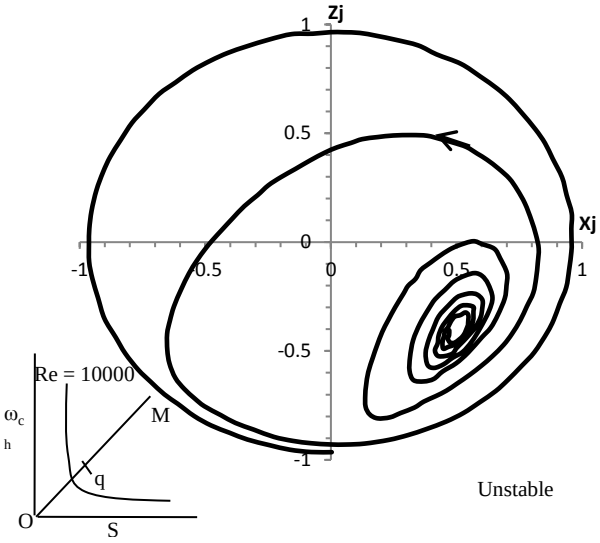

Fig. 30. Path of bearing shaft centre with Nonlinearity with fixed velocity along OM line (Re=10000, L/D = 0.5, S_n = 0.11, at point 'q'

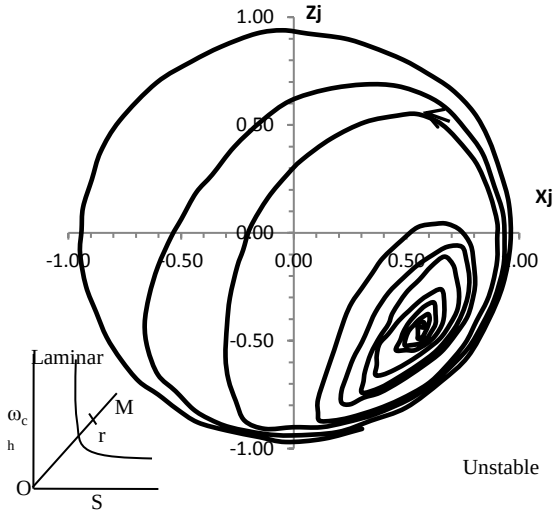

Fig. 31. Path of bearing shaft centre with Nonlinearity with fixed velocity along OM line, (Laminar flow, L/D = 0.5, S_n = 0.17, at point 'r')

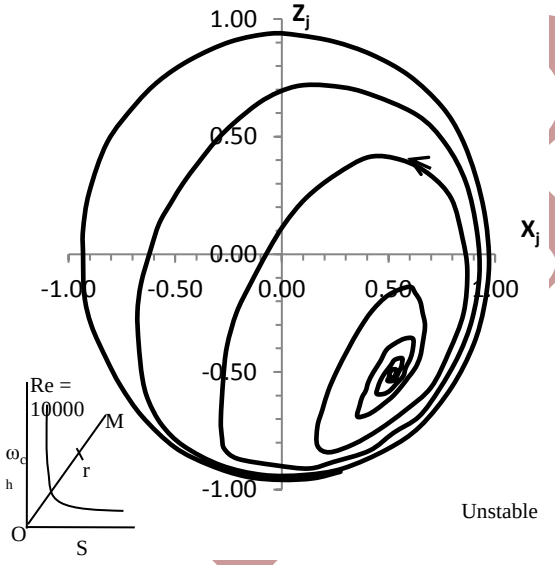

Fig. 32. Path of bearing shaft centre with Nonlinearity with fixed velocity along OM line, (Re = 10000, L/D = 0.5, S_n = 0.17, at point 'r')

5. Conclusion

A parametric study of lubricant supply conditions on the performance of non recessed hybrid journal bearings has been carried out using the analytical model. On the basis of proposed analytical analysis following conclusions are drawn:

i. Non-dimensional load capacity increases with increase in a/L(a/L) whereas it decreases with increase in w/D(w/D). The optimum dimension of groove for better static and dynamic characteristic of bearing were obtained as a/L = 0.8, w/D = 0.02 and Ist groove angle $\alpha_{1g} = 0^0$ (90^0 from load line).

ii. The location of the grooves with respect to the load line is found to affect strongly most performance parameters due to the strong interference of the grooves in the hydrodynamic pressure field. The optimum position was found between sixty degree and ninety degree ($\alpha_{1g} = 0^0$) to the load line.

iii. The stability of two grooved hybrid bearing reduces due to turbulence. The stability margin is reduced with increasing Reynolds number whereas stability charts shifts towards left side with increase Reynolds number.

References

[1] J. P. O'Donoghue, and W. B. Rowe, "Hydrostatic journal bearings (Exact Procedure)", *Tribology International*, Vol. 1, No. 4, pp. 230-236, (1968).

[2] J. P. O'Donoghue, and W. B. Rowe, "Hydrostatic journal design, *Tribology International*, Vol.2, No.1, pp.25-71, (1969).

[3] D. Koshal, and W. B. Rowe, "Fluid film journal bearings operating in hybrid mode: Part 1- Theoretical analysis and design", *Transaction of ASME*, Vol. 103, No. 4, pp. 558-565, (1981).

[4] D. Koshal, and W. B. Rowe,"Fluid film journal bearings operating in hybrid mode: Part II- Experimental

investigation", *Transaction of ASME, Journal of lubrication Technology*, Vol. 103, No. 4, pp. 566-572, (1981).

[5] L. San Andres, and A. Z. Szeri, Flow between eccentric rotating cylinders, *ASME J Appl Mechs*, Vol. 51, No. 4, pp. 869-878, (1984).

[6] M. H. Morton, P. G. Johnson, and J.H. Walton, "The influence of grooves in bearing on the stability and response of rotating systems", *Trib. Ser*., Vol. 11, No. 1, 347–354, (1987).

[7] M. K. Gethin, D. T. and Delhi El, "Effect of loading direction on the performance of a twin axial groove cylindrical bore bearing, *Trib. Int.*, Vol.20, No. 4, pp.179–185, (1987).

[8] R. Sinhasan and H. N. Chantrawat, "An elastohydrodynamic study on two-axial-groove journal bearing", *Tribology International*, Vol. 21, No. 6, pp. 341-351, (1988).

[9] R. Pai, and B. C. Mazumdar, "Stability of submerged oil journal bearings under dynamic load", *Wear*, Vol. 146, No. 1, pp. 125-135, (1991).

[10] J. M. McCormick and M.G.Salvadori, M.G., *Numerical methods in FORTRAN*, Prentice Hall of India, (1992).

[11] J. C. P. Claro, and A. A. S. Miranda, , "Analysis of hydrodynamic journal bearings considering lubricant supply condition", *Proc IMechE Part C: Journal of Mechanical Engineering Science*, Vol. 207, No. 1, pp. 93-101, (1993).

[12] A. Kumar, and S. S. Mishra, "Stability of a rigid rotor in turbulent hydrodynamic worn journal bearings", *Wear*, Vol. 193, No. 1, pp.25-30, (1996).

[13] A. Kumar, and S. S. Mishra, "Steady state analysis of noncircular worn journal bearings in non-laminar lubrication regimes", Tribology International, Vol.29, No. 6, pp.493-498, (1996).

[14] F. A. Martin, "Oil flow in plain steadily loaded journal bearings: Realistic predictions using rapid techniques, *Proc. Inst. Mech. Eng. Part J J. Eng. Tribol.* Vol.212, No. 6, pp. 413–425, (1998).

[15] S. K. KaKoty, and B. C. Mazumdar, "Effect of fluid inertia on stability of journal bearings", *ASME Journal of Tribology*, Vol. 122, No.4, pp. 741-745, (2000).

[16] C T. Jerry, and K. N. Su Lie, , "Rotation effects on hybrid hydrostatic/hydrodynamic journal bearings". *Industrial Lubrication and Tribology*, Vol. 53, No. 6, pp. 261 – 269, (2001).

[17] L. Costa, A. S. Miranda, M. Fillon, J. C. P. Claro, "An analysis of the Effect of oil supply conditions on the thermohydrodynamic performance of a single-groove journal bearing", Proc. Inst. Mech. Eng. *Part J, J. Eng. Tribol.*, Vol. 217, No. 2, pp. 133–144, (2003).

[18] B. C. Majumdar, R. Pai, and D. J. Hargreaves, "Analysis of water lubricated journal bearings with multiple and axial grooves", *Proc IMechE Part J: Journal of Engineering Tribology*, Vol. 218,

No. 2, pp.135-146, (2004).

[19] C. Desai, D. Patel, "Experimental analysis of pressure distribution of Hydrodynamic Journal Bearing: A parametric study", *Proc of Int. Conf. Mechanical Enineering*", pp.1-4 (2005)

[20] F. P. Brito, J. Bouyer, M. Fillon and A. S. Miranda, "Thermal behavior and performance characteristics of a twin axial groove journal bearing as a function of applied load and oil supply temperature", TRIBOLOGIA Finnish *J. Trib*. Vol. 3, No.1, pp.24–33, (2006).

[21] F. P. Brito, A. S. Miranda, J. Bouyer, M. Fillon, "Experimental Investigation of the Effect of Supply Temperature and Supply Pressure on the Performance of a Two-Axial Groove Hydrodynamic Journal Bearing", *J. Tribol.* Vol.129, No. 1, pp.98, (2007).

[22] L. Roy, and S. K. Laha, "Steady state and dynamic characteristics of axial grooved journal bearings", *Tribology International*, Vol.42, No. 5, pp. 754-761, (2009).

[23] R. R. Navthar, and N. V. Halegowda, "Stability Analysis of Hydrodynamic Journal Bearing using Stiffness", *Int. J. Engg. Sci. & Tech.*, Vol. 2, No. 2, pp.87–93, (2010).

[24] N. P. Mehta, S. S. Rattan, and R. Verma,"Stability analysis of two lobe hydrodynamic journal bearing with couple stress lubricant", *ARPN Journal of Engineering & Applied Science*, Vol. 5, No. 1, pp.69-74, (2010).

[25] M. V. Kini, R. S. Pai, D. S. Rao, S. B. Satish, R. Pai, "Effect of groove location on the dynamic characteristics of multiple axial groove water lubricated journal bearing", *World Acad. Sci. Eng. Technol.*, Vol. 60, pp.1592–1596, (2011).

[26] F.P. Brito, A.S. Miranda, J.C.P. Claro, M. Fillon, "Experimental comparison of the performance of a journal bearing with a single and a twin axial groove configuration", *Tribol. Int.*, Vol. 54, No.1, pp.1–8, (2012).

[27] L. Roy, S. K. Kakoty, "Optimum groove location of hydrodynamic journal bearing using genetic algorithm", *Adv. Tribol.* Vol. 2013. No.1, pp. 1-13 (2013).

[28] V. K. Dwivedi, S. Chand , K. N. Pandey, "Effect of Number and Size of Recess on the Performance of Hybrid (Hydrostatic/Hydrodynamic) Journal Bearing", *Proceedia Engineering*, Vol. 51, pp. 810-817, (2013).

[29] V. K. Dwivedi, S. Chand , K. N. Pandey, "Effect of Different Flow Regime on the Static and Dynamic Performance Parameter of Hydrodynamic Journal Bearing", *Proceedia Engineering*, Vol. 51, pp. 520-528, (2013).

[30] V. K. Dwivedi, S. Chand , K. N. Pandey, "Effects of turbulence on dynamic performance of accelerated / decelerated hydrodynamic journal bearing system", *Int. J. Design Engg.*, Vol. 5 No. 3, pp.256–288, (2014).

[31] F. P. Brito, A. S. Miranda, J. C. P. Claro, J. C. Teixeira, L. Costa, and M. Fillon,"Thermohydrodynamic modeling of journal bearings under

varying load angle and negative groove flow rate", *Proc IMechE Part J: Journal of Engineering Tribology*, Vol. 228, No. 9, pp. 955-973, (2014).

[32] V. K. Dwivedi, S. Chand , K. N. Pandey, "Stability Analysis of Twin Axial Groove Hybrid Journal Bearing", *J Appl. Fluid Mechs*, Vol. 9, No.6, pp. 2763-2768, (2016).

[33] S. Sharma, R. K. Awasthi, "Performance of hydrodynamic journal bearing operating under transient wear", *Mechanics and Mechanical Engineering*, Vol. 22, No. 1, pp. 153-170, (2018).

[34] J. Wang, J. Zhang, J. Lin and L. Ma. "Study on lubrication performance of journal bearing with multiple texture distributions", *Appl. Sci*., Vol. 8, No. 2, pp. 244-256, (2018).